On the analysis of two-dimensional distributions of experimental variables in heavy ion physics

D.V. Kamanin[*], Yu.V. Pyatkov[*,†], O.V. Falomkina[*,**], Yu.P. Pytyev[**], B.M. Herbst[‡] and W.H. Trzaska[§]

[*]*Joint Institute for Nuclear Research, 141980 Dubna, Moscow Region, Russia*
[†]*National Nuclear Research University MEPHI, 115409 Moscow, Russia*
[**]*Lomonosov Moscow State University, Physics Faculty, Computer Methods in Physics Division, 119899, Russia*
[‡]*University of Stellenbosch, Applied Mathematics, South Africa*
[§]*Department of Physics of University of Jyväskylä, Finland*

Abstract. We study the theoretical description of many nuclear reactions where the evolution of the nuclear system is described as a trajectory in multidimensional deformation space. We propose a strategy for revealing the trajectories in the space of experimental observables, at prescribed confidence levels.

Keywords: potential energy surface in the space of nuclear deformations, nuclear fission modes, morphological methods of image analysis
PACS: 25.70.Jj; 25.85.-w

In an earlier study we proposed a novel approach for extracting information from known mass-energy distributions of the nuclear reaction products by processing the $2D$ data directly [2]. A typical $M-E$ fragment distribution, for instance in the $^{233}U(n_{th},f)$ reaction, looks like at first sight like a smooth hill. Closer inspection shows that each $E = const$ slice of this distribution (see Fig. 1) is not absolutely smooth but rather display local irregularities (peaks), as indicated by the arrows.

The origin of the peaks becomes clear from the following considerations. The yield $Y(M|E)$ of the fission fragment (FF) with mass M at a fixed value of E is equal to,

$$Y(M|E) = \sum_{Z} Y(M,Z|E) \tag{1}$$

The marginalization in expression (1) is done over all possible values of the FF nuclear charge Z. Thus, the spectrum shown in Fig. 1 is a superposition of the partial mass spectra at fixed charges (so called isotope distributions) known from experiments [3]. Let us define the term: "fine structure" (FS). By definition, it is the local areas (peaks) of the $2D$ distribution indicating increased yields of FFs above a smooth background. As can be inferred from Fig. 1 the FS in this case is due to larger yields of the even-charged FFs. It is the well-known "odd-even staggering", based on proton pairing [1]. The peaks in the adjacent sections $E = \text{const}$ are correlated, forming regular structures on the $E-M$ plane in the form of ridges parallel to the E-axis [3]. Henceforth this structure will be referred to as "vertical ridges".

We pose the question, is there any fine structure in the FF mass-energy distribution, different from the vertical ridges produced by odd-even staggering and caused, conse-

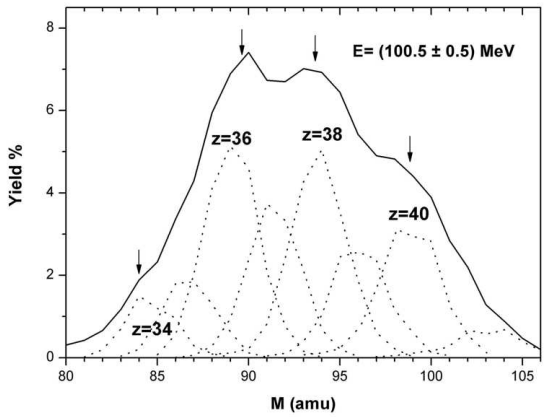

FIGURE 1. Section of the $E-M$ distribution for the energy of the fragment $E=(100.5\pm0.5)$ MeV [3]. The partial yields for the fixed nuclear charges are shown by dot lines.

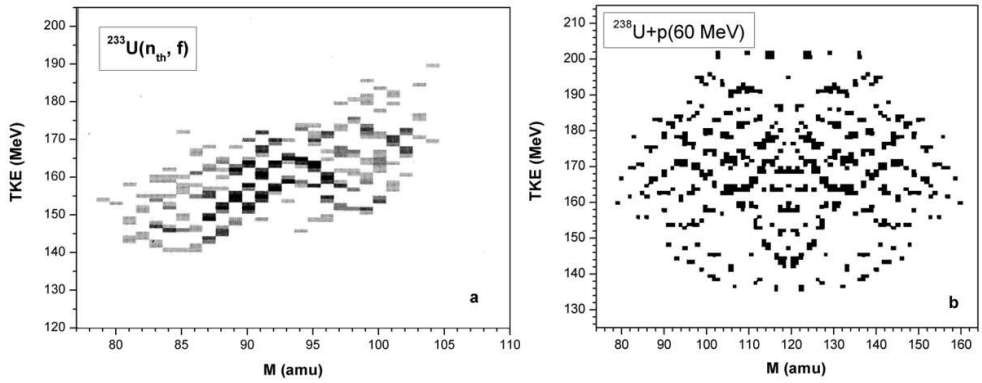

FIGURE 2. Snake-like FS exhibited by the TKE-M distributions of fragments from the reactions $^{233}U(n_{th},f)$ (a) and $^{238}U+p$ (60 MeV) (b). See text for details.

quently, by different physical processes? In order to automatically suppress the vertical ridges while searching for the fine structure, the sections $M=$ const are investigated, known to display local peaks [4, 5]. Methods based both on peak identification algorithms in gamma-ray spectroscopy and stochastic image processing are used in our investigations [2]. Fig. 2 shows examples of the FSs revealed in the total kinetic energy-mass (TKE-M) distributions of the fragments. Initial data were obtained using time-of-flights spectrometers described in [6, 7]. Darker points in the gray scale map (see Fig. 2a) correspond to higher intensities of the effect. Only the lighter mass peaks of the fission fragments are shown.

The symmetry shown in Fig. 2b is due to both the method of measurement of the fragment mass ("two velocities" method [1]), and the filter used [8].

Basically the FS represents a series of snake-like curves sometimes exhibiting bifurcation points [2, 8].

What are the reasons for investigating the specific FS observations? In the modern view, the evolution of the decaying nuclear system, for instance in fission, is mainly

determined by the potential energy of the system as a function of the parameters of its deformation or, in a $3D$ presentation by a potential energy surface (PES). Distinct potential valleys of the PES [11, 12] give rise to the preferable trajectories (realizations) of the system in the deformation space. As is shown by [13], at any point of the system's descent down the fission valley a scission can appear to occur, indicating a fission event in the space of experimental observables. In other words, the trajectories in the deformation space as a continuous sequence of nuclear states in the fission valley is mapped to continuous trajectories (smooth curves) in the plane of experimental observables [14], choosing the FF total kinetic energy and mass chosen variables in Fig. 2, for example. Thus we believe [15] the FS under discussion to be an image of the distinct fission process.

So far the weak point of the proposed data processing procedure is an absence of a quantitative confidence in the persistence of the extracted FS. Here the problem is exacerbated by the fact that we are looking for a new phenomenon, i.e. no prior knowledge about the shape of the structures is available.

In order to address this difficulty the following approach, based on the morphological methods of image analysis proposed in [9], is developed.

Let $\tilde{f}$ be an experimentally measured signal (i.e., the mass-energy distribution) that can be represented as follows

$$\tilde{f} = S + h + \nu, \tag{2}$$

where S is the image of a smooth "substrate", h a signal that might contain several instances of FSs, and ν additive noise (i.e. generated by some probability density function). At the first stage, the smooth underlying substrate S is extracted from the signal $\tilde{f}$, yielding $f = h + \nu$. Different methods can be used to extract S, using spline interpolation for example [2, 16]. During the second stage, the FS is extracted from the signal f, using methods based on morphological image analysis.

Let us briefly recall some of the definitions of morphological image analysis. An *image* $f(\cdot)$ is a square-integrable, integer valued function on a subset X of the Euclidean plane $\mathscr{R}^2$. X is called the *field of vision*, with $f(x)$ the brightness of the point $x \in X$. In the case under consideration $X = \{x_1, \ldots, x_n\}$, and the images $\tilde{f}(\cdot)$ $f(\cdot)$, $S(\cdot)$, $h(\cdot)$, and $\nu(\cdot)$ of (2) are defined at exactly the same points and are considered to be the elements of the Euclidean plane $\mathscr{R}^n$. The measurement error $\nu \in \mathscr{R}^n$ is considered to be a random image having zero mean, $\mathbf{E}\nu = 0$, and covariance matrix $\sigma^2 I$, where $I \in (\mathscr{R}^n \to \mathscr{R}^n)$ is the identity matrix, with σ^2 unknown.

The image of the FS is written as $\omega(\cdot)$ and is defined on a variable shape, variable size subset Ω of the field of vision X. Let us define the *shape* of the image $\omega(\cdot)$, as the set of images

$$V_\omega = \{\omega(\cdot), \omega(x) = c_1 \chi_{A_1}(x) + c_2 \chi_{A_2}(x),\ \ c_1 \geq c_2,\ \ c_1, c_2 \in \mathscr{R}_1,\ \ x \in \Omega\}, \tag{3}$$

with

$$\chi_{A_i}(x) = 1,\ \ x \in A_i;\ \ \textit{and}\ \ \chi_{A_i}(x) = 0,\ \ x \notin A_i;\ \ (i = 1, 2)$$

V_ω is a convex closed cone in $\mathscr{R}^2$ and in $\mathscr{R}^n$. In this definition A_1 and A_2 are different regions of Ω of constant brightness. According to this definition, the *shape* of the image of an object therefore consists of all images of the object that differ in brightness in regions of Ω of constant brightness.

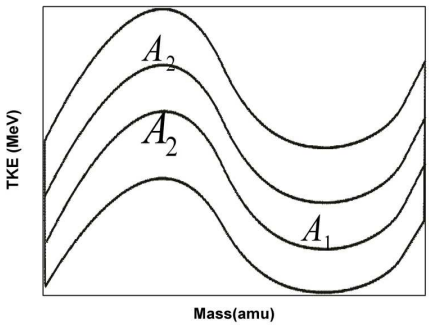

FIGURE 3. Example of regions $A_1, A_2 \subset \Omega$ of constant brightness of an image of the FS

In Fig. 3 regions $A_1, A_2 \subset \Omega$ of constant brightness of a FS image are shown. In this figure, the field of vision is split into regions A_1, A_2, with A_1 the "fine structure" itself, and A_2 the surrounding region. The shape (in the usual sense) and the size of the regions A_1 and A_2 are defined by the researcher. Note that the expected shape is postulated by the user, this procedure returns the confidence in the actual presence of the shape in the image. In our case the the postulated shape is derived from Fig. 2. The brightness of regions A_1 and A_2 are supposed to remain constant. The fact that the brightness at points that belong to the "fine structure" is greater than at surrounding points is reflected by the condition $c_1 \geq c_2$ in (3).

The projection P, defined below, of some image $g(\cdot)$ defined on Ω, onto the shape V_ω is the image $(P_{V_\omega} g)(\cdot)$. It exists and is unique, because V_ω is convex closed cone (see [9]),

$$(P_{V_w} g)(x) = \hat{c}_1 \chi_{A_1}(x) + \hat{c}_2 \chi_{A_2}(x),\ x \in \Omega, \tag{4}$$

where $\hat{c}_1, \hat{c}_2$ are the solutions of the following minimization problem,

$$\int_\Omega (g(x) - \hat{c}_1 \chi_{A_1}(x) - \hat{c}_2 \chi_{A_2}(x))^2 dx = \min_{c_1, c_2 \in \mathscr{R}_1 c_1 \geq c_2} \int_\Omega (g(x) - c_1 \chi_{A_1}(x) - c_2 \chi_{A_2}(x))^2 dx \tag{5}$$

We now consider the problem of FS extraction within the framework of the above formulated signal registration model as a statistical hypothesis testing problem, H – for image f there exists a fragment f_ω, represented as

$$H : \exists f_\omega = g + \nu,\ \exists t \in T,\ g \in t(V_\omega),\ \nu \in (0, \sigma^2 I),\ \sigma^2 > 0,\ \|\nu\|^2 << \|g\|^2, \tag{6}$$

where the shape of g, up to translation and scaling coincide with (3), and $t \in T$ is a translation and scaling transformation with T the set of all such transformations. The alternative hypothesis K simply states: such a fragment does not exist.

To solve this hypothesis testing problem the following functional is used [9],

$$j(z) = \frac{||(I - P_{V_\omega}) z||^2}{||(P_{V_\omega} - P_{V_U}) z||^2}. \tag{7}$$

where z is the image under consideration, $P_{V_U} z$ is a projection of the image $z(\cdot)$ onto the shape U of the uniform field of vision,

$$U = \{u(\cdot), u(x) = \text{ const} \cdot \chi_\Omega(x),\ x \in \Omega\}. \tag{8}$$

The functional (7) has following properties:

1. Assume that the fragment f_ω exists and satisfies the condition (6), but cannot be represented as

$$f_\omega = g + \nu, \exists t \in T,\ g \in t(U), \nu \in (0, \sigma^2 I),\ \sigma^2 > 0. \tag{9}$$

   The numerator in (7) equals $||(I - P_{V_\omega})\nu||^2$, the denominator equals $||(P_{V_\omega} - P_{V_U})\nu + (P_{V_\omega} - P_{V_U})g||^2$ and has values of $O(\|g\|^2)$. Thus the value of the functional (7) is small, because $\|\nu\|^2 << \|g\|^2$.
2. Assume that the fragment f_ω exists and satisfies the condition (9). In this case the numerator in (7) equals $||(I - P_{V_\omega})\nu||^2$ and has values of $O(\|\nu\|^2)$. The denominator equals $||(P_{V_\omega} - P_{V_U})\nu||^2$ and also has values of $O(\|\nu\|^2)$. The functional $j(z)$ is therefore $O(1)$.
3. Assume that the fragment f_ω satisfying the condition (6) or (9) does not exist. The numerator in (7) equals $||(I - P_{V_\omega})\nu + (I - P_{V_\omega})g||^2$ and is of $O(\|g\|^2)$. The denominator, which equals $||(P_{V_\omega} - P_{V_U})\nu + (P_{V_\omega} - P_{V_U})g||^2$, is also of $O(\|g\|^2)$, and again the functional $j(z)$ is $O(1)$.

Hence, only in the first case is the value of the functional (7) small, because $\|\nu\|^2 << \|g\|^2$.

The decision rule is as follows: hypothesis H is accepted if by means of translation and scaling, a fragment f_ω, such that $j(f_\omega) \leq A$ can be found, where A is a constant empirically determined, as explained below. Otherwise H is declined.

The value of the functional (7) is considered as a measure of the closeness between image z and the image with shape (3). Note that the functional (7) is invariant with respect to variations of the image's brightness and contrast values, i.e. to transformations $z \to \alpha z + \beta$, where α is a number, and β is an image defined on Ω.

The value of the constant A is defined as follows. First of all using experimental data the value of A determined that appears acceptable for an image of the proposed FS. A value of $A = 40$ appears to be appropriate. The reliability of this value is verified by means of experiments on synthetic data. We use 10000 synthetic images of smooth substrates S with additive Poisson-distributed noise. The noise parameters were the same as in real experiment. The methods that have been proposed in [2, 16] are used to remove the noise from the smooth substrate. Subsequently an empirical distribution of the values of the functional (7) at the specified noise levels is determined. Based on this distribution the probability is estimated as $P(j \leq A) = 0.001$, see Fig. 4. This is the probability of erroneously accepting the hypothesis against the closest alternative, "uniform field of vision". According to the properties of the functional (7), this probability estimates an upper bound for the probability of erroneously accepting the hypothesis against the alternative, "fragment does not exist". This criterion is analogous to the principle of the locally uniformly of the most powerful criterion [17].

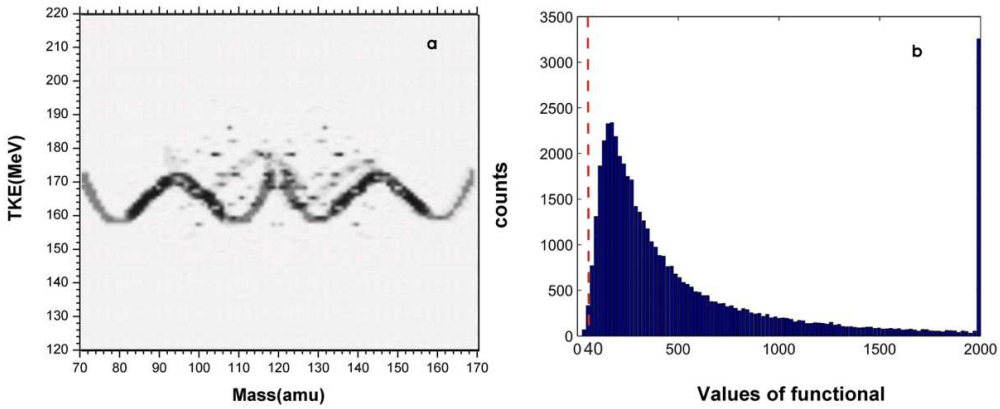

FIGURE 4. (a) The fine structure revealed at the same TKE-M distribution, as is shown at Fig. 2 (b). (b) The spectrum of functional (7) values, obtained based on model data. The dotted line shows the threshold value A, for which $P(j \leq A) = 0.001$.

According to this statistical analysis, the probability that the "fine structure" obtained from real experimental data is due to noise, is small. Fig. 4a) shows the result of the "fine structure" extracted from real experimental data using the method described above, as compared with the result obtained earlier in Fig. 2b).

The proposed method enables one to search for structures that have different shapes, and should also be useful in other contexts.

In summary, we emphasize the two main aspects of this approach to the analysis of two-dimensional distributions of experimental observables originated from nuclear reactions.

1. Multi-valley structures of the potential energy surface of nuclear system, at least in fusion, fission and quasifission reactions, describe different discrete reactions along these valleys. Each reaction manifests itself as a trajectory in the space of experimental observables such as mass-asymmetry and total kinetic energy, coupled with prescession elongation of the system. Visualization of these trajectories (revealing the fine structure) can give access to unique physical information, unknown in the past.
2. In order to obtain quantitative estimates of our confidence in the extracted structures, we developed a mathematical approach based on morphological methods of image analysis. Within its framework, one estimates the probability of random (due to the noise) realizations of the structure (or its scaled versions). This provides necessary confidence in the observations for subsequent physical analysis.

REFERENCES

1. The Nuclear Fission Process, edited by Cyriel Wagemans, CRC Press, 1991.
2. Yu. V. Pyatkov et al., *Nucl. Instr. and Methods A* **488**, 381–399 (2002).
3. U. Quade et al., *Nucl. Phys. A* **487**, 1–36 (1988).
4. M. N. Rao et al., *Nucl. Instr. and Methods A* **313**, 227–232 (1992).

5. T. Ohtsuki et al., *Phys. Rev. Lett.* **66**, 17–20 (1991).
6. A. A. Alexandrov et al., *Nucl. Instr. and Methods A* **303**, 323–331 (1991).
7. W. H. Trzaska et al., cP 392, AIP Press, p.1059, (1997).
8. W. H. Trzaska et al., *Proc. Symposium on Nuclear Clusters, Rauischholzhausen, Germany* 2002, pp. 237-242.
9. Yu. P. Pytyev, Morphological Image Analysis in *Pattern Recognition and Image Analysis*. Vol. 3, No. 1, 1993, pp. 19–28.
10. O. V. Falomkina et al., Heavy Ion Physics, FLNR JINR Scientific Report 2001-2002, Dubna 2003, pp. 149–150.
11. V. V. Pashkevich, *Nucl. Phys. A* **169**, 275–293 (1971).
12. U. Brosa et al., *Phys. Rep.* **197**, 167–262 (1990).
13. J. F. Berger et al., *Nucl. Phys. A* **428**, 23–36 (1984).
14. Yu. V. Pyatkov et. al., *Nucl. Phys. A* **624**, 140-156 (1997).
15. Yu. V. Pyatkov et al., *Phys. of Atomic Nuclei* **67**, 1726-1730 (2004).
16. O. V. Falomkina et al., Heavy Ion Physics, FLNR JINR Scientific Report 2003 - 2004, Dubna, Russia, 2006, pp. 158–159.
17. C. R. Rao (chief ed.). Handbook of Statistics, Vols 1-18. New York and Amsterdam: North Holland/Elsevier Science Publishers.